

TABLE OF CONTENTS

	Page
ACKNOWLEDGEMENTS	iii
ABSTRACT (ENGLISH)	v
ABSTRACT (THAI)	vii
LIST OF TABLES	xiii
LIST OF FIGURES	xvii
ABBREVIATIONS AND SYMBOLS	xxiii
CHAPTER 1 INTRODUCTION	1
Research objectives	6
CHAPTER 2 LITERATURE REVIEW	7
2.1 Electronic properties of semiconductors	7
2.1.1 Band structure	7
2.1.2 Equilibrium carrier concentrations	20
2.1.3 Light absorption	24
2.1.4 Luminescence and light emission in solid	28
2.1.5 Interband luminescence of direct gap materials	30
2.1.6 Photoluminescence of direct gap materials	32
2.1.7 Photoluminescence for low carrier densities	35
2.2 Physics of solar cell	36
2.2.1 Basic structures for photovoltaic action	39

2.2.2 PN-junction	43
2.3 Dye-sensitized solar cells (DSSCs)	46
2.3.1 Materials and structure of DSSCs	48
2.3.2 The mechanism of the DSSCs	48
2.4 J-V measurement	53
2.5 Dielectric heating with microwave energy	54
2.5.1 Dielectric heating	55
2.5.2 Effect of the loss factor	58
2.5.3 Penetration depth	58
2.5.4 Microwave plasma	59
2.5.5 RF and microwave discharge	60
2.5.6 Microwave plasma source	62
2.5.6 Generation of a plasma by microwave	63
2.6 Properties and synthesis of cadmium sulfide (CdS)	69
2.7 Properties and synthesis of cadmium telluride (CdTe)	76
2.8 Properties and synthesis of zinc telluride (ZnTe)	77
2.9 Properties and synthesis of zinc oxide (ZnO)	84
CHAPTER 3 EXPERIMENTAL PROCEDURE	85
3.1 Chemical reagents and equipments	85
3.1.1 Chemical reagents	85
3.1.2 Equipments and instruments	86
3.2 Synthesized methods	87
3.2.1 Synthesis of CdS using microwave plasma	87
3.2.2 Synthesis of CdTe using microwave plasma	88

3.2.3 Synthesis of ZnTe using microwave plasma	89
3.2.4 Synthesis of ZnO using microwave plasma	90
3.2.5 Synthesis of ZnO using using sonochemical process	90
3.3 Characterization	91
3.3.1 X-ray diffraction (XRD)	91
3.3.2 Scanning electron microscope (SEM) and energy dispersive X-ray analyser	92
3.3.3 Transmission electron microscope (TEM)	93
3.3.4 Luminescence spectrometer	94
3.3.5 UV-Vis-NIR spectrophotometer	95
3.3.6 Raman spectrometer	96
3.3.7 Solar simulator	97
CHAPTER 4 RESULTS AND DISCUSSION	98
4.1 CdS synthesized by a microwave plasma technique	98
4.2 CdTe synthesized by a microwave plasma technique	118
4.3 ZnTe synthesized by a microwave plasma technique	130
4.4 ZnO film on FTO for DSSCs synthesized by a microwave plasma technique	143
4.5 CdTe-GPE composited electrolyte on quasi solid-state ZnO Based dye-sensitized solar cells	145
4.6 ZnTe-GPE composited electrolyte on quasi solid-state ZnO Based dye-sensitized solar cells	148
CHAPTER 5 CONCLUSIONS	152
REFERENCES	155

APPENDICES	168
APPENDIX A Analytical equipments	169
APPENDIX B Camera constants used for the indexing of SAED pattern	172
APPENDIX C Microwave induced plasma system	173
APPENDIX D International publications	174
CURRICULUM VITAE	187

LIST OF TABLES

Table		Page
4.1	Calculated lattice parameter of CdS from the experiment (molar ratio of Cd:S=1:2, 100 min), comparing with the JCPDS file (Reference code: 06-0314 [110] for CdS)	101
4.2	Calculated lattice parameter of CdS from the experiment (molar ratio of Cd:S=1:2, 120 min), comparing with the JCPDS file (Reference code: 06-0314 [110] for CdS)	102
4.3	Calculated lattice parameter of CdS from the experiment (molar ratio of Cd:S=1:2, 140 min), comparing with the JCPDS file (Reference code: 06-0314 [110] for CdS)	103
4.4	The 2θ diffraction angles and intensities of the JCPDS no. 06-0314 and for the 1:2 molar ratio of Cd:S and 100 min product obtained from the experiment and simulation.	104
4.5	The 2θ diffraction angles and intensities of the JCPDS no. 06-0314 and for the 1:2 molar ratio of Cd:S and 120 min product obtained from the experiment and simulation.	105
4.6	The 2θ diffraction angles and intensities of the JCPDS no. 06-0314 and for the 1:2 molar ratio of Cd:S and 140 min product obtained from the experiment and simulation.	106

4.7	Crystallinities percentage of 1:2 molar ratio for 100, 120, 140 min and standard values.	107
4.8	The crystallite size (D) of 1:2 molar ratio CdS for 100, 120 and 140 min products calculated from the scherrer's formula and the full width at half maximum (FWHM) of the XRD spectra	109
4.9	Ring diffraction pattern values of 1:2 molar ratio CdS produced for 100 min, and the parameters of the JCPDS standard.	116
4.10	Ring diffraction pattern values of 1:2 molar ratio CdS produced for 120 min, and the parameters of the JCPDS standard.	117
4.11	Calculated lattice parameter of CdTe from the experiment (molar ratio of Cd:Te=1:1, 10 min), comparing with the JCPDS file (Reference code: 15-0770 [110])	120
4.12	Calculated lattice parameter of CdTe from the experiment (molar ratio of Cd:Te=1:1, 20 min), comparing with the JCPDS file (Reference code: 15-0770 [110])	120
4.13	Calculated lattice parameter of CdTe from the experiment (molar ratio of Cd:Te=1:1, 30 min), comparing with the JCPDS file (Reference code: 15-0770 [110])	121
4.14	The 2θ diffraction angles and intensities of the JCPDS no. 15-0770 of Cd:Te, 900W and 10 min product obtained from the experiment and simulation.	121
4.15	The 2θ diffraction angles and intensities of the JCPDS no. 15-0770 of Cd:Te, 900W and 20 min product obtained from the experiment and simulation.	122

4.16	The 2θ diffraction angles and intensities of the JCPDS no. 15-0770 of Cd:Te, 900W and 30 min product obtained from the experiment and simulation.	122
4.17	Crystallinities percentage of 1:1 molar ratio for 10, 20, 30 min and standard values.	123
4.18	The crystallite size (D) of 1:2 molar ratio CdTe for 10, 20 and 30 min products calculated from the scherrer's formula and the full width at half maximum (FWHM) of the XRD spectra	123
4.19	Ring diffraction pattern values of 1:1 molar ratio CdTe produced for 10 min, and the parameters of the JCPDS standard.	124
4.20	Ring diffraction pattern values of 1:1 molar ratio CdTe produced for 30 min, and the parameters of the JCPDS standard.	125
4.21	Calculated lattice parameter of ZnTe from the experiment (molar ratio of Zn:Te = 1:1, 600 watt.) comparing with the JCPDS file (15-0746)	132
4.22	Calculated lattice parameter of ZnTe from the experiment (molar ratio of Zn:Te = 1:1, 900 watt.) comparing with the JCPDS file (15-0746)	132
4.23	The 2θ diffraction angles and intensities of the JCPDS no. 15-0746 of Zn:Te, 600W for 30 min product obtained from the experiment and simulation.	133
4.24	The 2θ diffraction angles and intensities of the JCPDS no. 15-0746 of Zn:Te, 900W for 30 min product obtained from the experiment	133

4.25	The crystallite size (D) of 1:1 molar ratio ZnTe for 30 min products calculated from the scherrer's formula and the full width at half maximum (FWHM) of the XRD spectra	134
4.26	Ring diffraction pattern values of ZnTe produced under the 1:1 molar ratio of Zn:Te, 600W and 30 min condition, and the parameters of the JCPDS standard.	137
4.27	Ring diffraction pattern values of ZnTe produced under the 1:1 molar ratio of Zn:Te, 900W and 30 min condition, and the parameters of the JCPDS standard.	138
4.28	Voc, Jsc, ff and η for different wt% CdTe-GPE	147
4.29	Voc, Jsc, ff and η for different wt% ZnTe-GPE	150

LIST OF FIGURES

Figure		Page
2.1	Schematic band diagrams for the photoluminescence processes in a direct gap material (left) and an indirect gap material (right)	13
2.2	A simplified energy band diagram at $T > 0$ K for a direct band gap (E_g)	19
2.3	The Fermi function at various temperatures	20
2.4	Donor and acceptor levels in a semiconductor.	23
2.5	Photon absorption in a direct band gap semiconductor for an incident photon with energy $h\nu > E_g$	25
2.6	Photon absorption in an indirect band gap semiconductor for a photon with energy $h\nu < E_2 - E_1$ and a photon with energy $h\nu > E_2 - E_1$. Energy and momentum in each case are conserved by the absorption and emission of a phonon, respectively	27
2.7	General scheme of luminescence in a solid	29
2.8	The interband luminescence process in a direct gap semiconductor	31
2.9	The processes occurring during photoluminescence in a direct gap semiconductor after excitation at frequency ν_L	33
2.10	A schematic of a simple conventional solar cell. Creation of electron-hole pairs, e^- and h^+ , respectively, is depicted	37
2.11	The radiation spectrum for a black body at 5762 K, an AM0 spectrum, and an AM1.5 global spectrum	39

- 2.12 (a) Two semiconductors prior to contact, (b) the same two semiconductors during contact and (c) the same two semiconductors after contact, in thermodynamic equilibrium. 41
- 2.13 Equilibrium conditions in a solar cell: (a) energy bands; (b) electric field; and (c) charge density 45
- 2.14 Operation mechanism of the dye sensitized electrochemical solar cell (DSSCs). D: Dye, O: Oxidant (e.g, I_3^-), R: Reductant (e.g. I^-). (a) Wet-type DSSC with redox couple in the liquid electrolyte (b) Solid state DSSCs with a p-type semiconductor to replace the electrolyte containing the redox couple. 47
- 2.15 The DSSCs mechanism for generating electric power. 50
- 2.16 The current density-voltage curve. In this, point of maximum output power is found. 53
- 2.17 (a) Dipole rotations of molecule occurs in materials containing polar molecules having an electrical dipole moment, which will align molecules in a microwave electromagnetic field. 55
- (b) Molecular rotation for the generation of energy in the form of microwave electromagnetic radiation.
- 2.18 Power flow when an electromagnetic wave strikes a dielectric material with high loss factor 58
- 2.19 Schematic diagram of Cober microwave system used in the synthesis of binary nitride materials by exposing in a nitrogen plasma. 65

2.20	Schematic diagram of (a) the apparatus for plasma modification by making use of an atmospheric microwave plasma torch, and (b) the construction of the plasma nozzles.	67
2.21	A schematic diagram of microwave plasma equipment.	68
2.22	The properties and structure of CdS (wurtzite)	69
2.23	The properties and structure of CdTe (cubic)	76
2.24	The properties and structure of ZnTe (cubic)	78
2.25	The ZnTe applications (a) semiconductor diodes, (b) electro-optics, (c) solar cells, (d) assorted discrete transistors and (e) light-emitting diodes (LED).	79
2.26	The properties and structure of ZnO (wurtzite)	84
3.1	Schematic diagram of microwave induced plasma system.	88
3.2	X-ray diffractometer.	92
3.3	Scanning electron microscope.	93
3.4	Transmission electron microscope.	94
3.5	Luminescence spectrometer.	95
3.6	UV-Vis-NIR Spectrophotometer.	95
3.7	Raman spectrometer.	97
3.8	Solar simulator.	97
4.1	(a) XRD patterns of CdS synthesized using power 900W and different Cd:S molar ratios for 20 min	98
4.1	(b) XRD patterns of CdS synthesized using power 900W, 1:2 molar ratio of Cd:S and different lengths of time for heating by microwave plasma.	99

4.2	Particles sizes of CdS synthesized using (a) different molar ratio at 20 min (b) different lengths of time for heating at 1:2 molar ratio.	108
4.3	Raman spectra of 1:2 molar ratio CdS synthesized for 120 min and 140 min.	110
4.4	SEM image and clusters sizes of 1:2 molar ratio CdS product for 120 min	111
4.5	SEM image and clusters sizes of 1:2 molar ratio CdS product for 140 min	112
4.6	Photoluminescence of CdS produced under the 1:2 molar ratio of CdS condition	114
4.7	The $(\alpha h\nu)^2$ versus $h\nu$ plots of CdS synthesized by the solid state microwave-plasma for 120 and 140 min	115
4.8	TEM image (a), and SAED pattern(b) of 1:2 molar ratio CdS produced for 100 min.	116
4.9	TEM image (a), and SAED pattern(b) of 1:2 molar ratio CdS produced for 120 min.	117
4.10	XRD patterns of CdTe synthesized using different 1:1(Cd:Te) molar ratios for 10, 20 and 30 min	118
4.11	TEM images (a) and ED patterns (b) of CdTe synthesized via the 900W microwave plasma for 10 min.	124
4.12	TEM images (a) and ED patterns (b) of CdTe synthesized via the 900W microwave plasma for 30 min.	125
4.13	SEM image and clusters sizes of 1:1 molar ratio CdTe product for 10 min	126

4.14	SEM image and clusters sizes of 1:1 molar ratio CdTe product for 20 min	126
4.15	SEM image and clusters sizes of 1:1 molar ratio CdTe product for 30 min	127
4.16	Raman spectra of CdTe synthesized under microwave power at 900 watt various the length of time for heating on 10, 20 and 30 min	128
4.17	The $(\alpha h\nu)^2$ versus $h\nu$ plots of CdTe synthesized under various of length of time on 10 and 30 min	129
4.18	XRD patterns of ZnTe synthesized using different 1:1(Zn:Te) heating power for 300, 450, 600 and 900 W for 30 min.	131
4.19	SEM image and clusters sizes of 600W and 1:1 molar ratio ZnTe product for 30 min at x20,000 (a) x50,000 (b)	135
4.20	SEM image and clusters sizes of 900W and 1:1 molar ratio Zn:Te product for 30 min at x5,000 (a) x20,000 (b)	136
4.21	SAED pattern of ZnTe produced under the 1:1 molar ratio of Zn:Te condition (a) 600 W (b) 900 W	137
4.22	Photoluminescence of ZnTe produced under various of microwave power at 600 and 900 watt	139
4.23	The $(\alpha h\nu)^2$ versus $h\nu$ plots of ZnTe synthesized under various of microwave power at 600 and 900 watt	140
4.24	Raman spectra of ZnTe synthesized under various of microwave power at 300, 450, 600 and 900 watt	141
4.25	SEM images 600 W (a) 900 W (b) SAED patterns of ZnTe synthesized via the 900W microwave plasma for 30 min (c) simulation	142

4.26	XRD patterns of (a) deposit ZnO thin film on FTO, (b) calcinations of porous Zn film to porous ZnO film, (c) FTO	143
4.27	FE-SEM image of ZnO particles that deposited on FTO	144
4.28	The flow chart for preparation the p-CdTe gel polymer composite electrolyte	145
4.29	A schematic diagram of the CdTe-GPE-DSSC	146
4.30	The simplified energy level diagram of the CdTe-GPE-DSSC	146
4.31	J-V characteristic curves of DSSCs for different wt % CdTe-GPE electrolyte.	147
4.32	The flow chart for preparation the p-ZnTe-GPE	148
4.33	A schematic diagram of the ZnTe-GPE-DSSC	149
4.34	The simplified energy level diagram of the ZnTe-GPE-DSSC	149
4.35	J-V characteristic curves of DSSCs for different wt % CdTe-GPE	150

ABBREVIATIONS AND SYMBOLS

Physical constants

Avogadro constant, N_A	=	6.022×10^{23}	mol^{-1}
Boltzmann constant, k	=	1.3806×10^{-23}	J K^{-1}
Elementary charge, e	=	1.602×10^{-19}	C
Electron mass, m_e	=	9.109×10^{-31}	kg
Planck constant, h	=	6.626×10^{-34}	J s
Vacuum permittivity, ϵ_0	=	8.854×10^{-12}	F m^{-1}
Velocity of light, c	=	2.998×10^8	m s^{-1}
1 electron volt, 1eV	=	1.602×10^{-19}	J

Physical variables

ν = Frequency

ω = Angular frequency

ω_c = Plasma frequency

λ = Wavelength

k = Wave vector

m^* = Effective mass

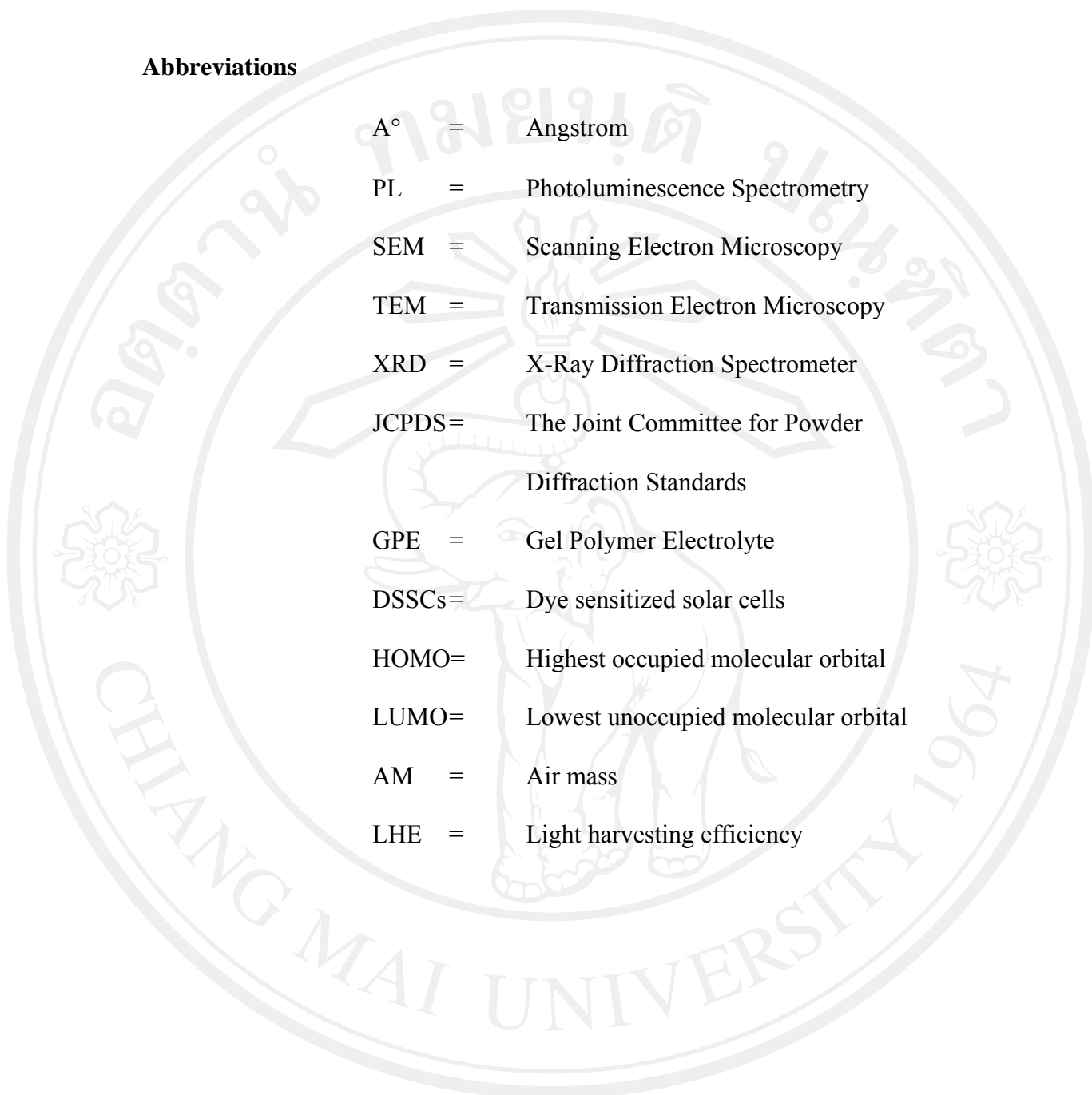
m_e^* = Electron effective mass

m_h^* = Hole effective mass

ff = Fill factor

η = Energy conversion efficiency

J_{sc}	=	Short circuit current density
V_{oc}	=	Open circuit voltage
P_{in}	=	Incident light power
P_{max}	=	Maximum power output
V_{max}	=	Maximum photovoltage
E_g	=	Energy band gap
E_F	=	Fermi energy
$g_c(E)$	=	Density of states in the conduction band
$g_v(E)$	=	Density of states in the valence band
n_0	=	Electron concentrations
p_0	=	Hole concentrations
N_C	=	Conduction-band effective densities of state
N_V	=	Valence-band effective densities of state
n_i	=	Intrinsic carrier concentration
E_i	=	Fermi energy in an intrinsic semiconductor
χ	=	Electron affinity
ϕ	=	Work function
V_{bi}	=	Built-in potential
W_D	=	Depletion width
ϵ'	=	Relative permittivity or dielectric constant
θ_A	=	Mean power transfer per electron
δ	=	Loss angle
E_{rms}	=	Root-mean-square electric field

AbbreviationsThe background of the page features a large, light gray watermark of the Chiang Mai University logo. The logo is circular and contains a central figure of a mythical creature (Garuda) holding a sword and a shield. The text "มหาวิทยาลัยเชียงใหม่" is written in Thai script around the top inner edge, and "CHIANG MAI UNIVERSITY 1964" is written in English around the bottom inner edge.

A°	=	Angstrom
PL	=	Photoluminescence Spectrometry
SEM	=	Scanning Electron Microscopy
TEM	=	Transmission Electron Microscopy
XRD	=	X-Ray Diffraction Spectrometer
JCPDS	=	The Joint Committee for Powder Diffraction Standards
GPE	=	Gel Polymer Electrolyte
DSSCs	=	Dye sensitized solar cells
HOMO	=	Highest occupied molecular orbital
LUMO	=	Lowest unoccupied molecular orbital
AM	=	Air mass
LHE	=	Light harvesting efficiency